nature geoscience

ARTICLES

PUBLISHED ONLINE: 6 FEBRUARY 2017 | DOI: 10.1038/NGEO2891

Warm Mediterranean mid-Holocene summers inferred from fossil midge assemblages

Stéphanie Samartin[1,2], Oliver Heiri[1,2]*, Fortunat Joos[1,3], Hans Renssen[4,5], Jörg Franke[1,6], Stefan Brönnimann[1,6] and Willy Tinner[1,2]

Understanding past climate trends is key for reliable projections of global warming and associated risks and hazards. Uncomfortably large discrepancies between vegetation-based summer temperature reconstructions (mainly based on pollen) and climate model results have been reported for the current interglacial, the Holocene. For the Mediterranean region these reconstructions indicate cooler-than-present mid-Holocene summers, in contrast with expectations based on climate models and long-term changes in summer insolation. We present new quantitative and replicated Holocene summer temperature reconstructions based on fossil chironomid midges from the northern central Mediterranean region. The Holocene thermal maximum is reconstructed 9,000–5,000 years ago and estimated to have been 1–2 °C warmer in mean July temperature than the recent pre-industrial period, consistent with glacier and marine records, and with transient climate model runs. This combined evidence implies that widely used pollen-based summer temperature reconstructions in the Mediterranean area are significantly biased by precipitation or other forcings such as early land use. Our interpretation can resolve the previous discrepancy between climate models and quantitative palaeotemperature records for millennial-scale Holocene summer temperature trends in the Mediterranean region. It also suggests that pollen-based evidence for cool mid-Holocene summers in other semi-arid to arid regions of the Northern Hemisphere may have to be reconsidered, with potential implications for global-scale reconstructions.

For the late Quaternary, millennial-scale quantitative records of temperature changes on landmasses are to a large extent based on evidence of past vegetation change, specifically pollen records from lake and peat sediments[1–3]. Recent vegetation-based temperature reconstructions, mainly from regions with seasonally or annually arid climate, have suggested that large parts of the northern mid-latitudes may have been characterized by cooler mid-Holocene summer temperatures than observed in the latest Holocene and at present[1,3,4] rather than by a mid-Holocene thermal maximum (HTM) as expected based on variations in summer insolation and key non-quantitative palaeoclimate records from the northern temperate, subarctic and arctic region[5]. Cooler mid than late Holocene summer temperatures in these regions would contradict the predictions of climate models for regional millennial-scale Holocene temperature development[6–8]. For example, in Europe a Holocene thermal minimum in the Mediterranean region, as suggested by some vegetation-based reconstructions[1,3,4], would contrast with warmer mid-Holocene summer temperatures in mid and high latitudes and imply major changes in latitudinal summer temperature gradients that climate models do not represent. It has been suggested that this disagreement points towards fundamental flaws in climate models and in our understanding of the drivers of late Quaternary climate change[9]. However, proxy–climate model discrepancies relying on single proxy types can, in some instances, be resolved by critically re-examining proxy calibration and interpretation[10], ideally together with new palaeotemperature evidence relying on fundamentally different, independent proxy–temperature relationships.

For the European Mediterranean region discrepancies between vegetation-based proxies and climate model predictions are particularly pronounced[6,7,9]. This raises questions about the applicability of climate models for predicting future temperature change in this region, which has been identified as exceptionally vulnerable to the consequences of future climatic change such as aridification, salinization, fire increase, soil erosion and biodiversity losses[11,12]. Vegetation-independent and quantitative reconstructions of millennial-scale summer temperature trends from landmasses in the Mediterranean region are lacking at present. Such reconstructions could be directly compared with pollen- and climate model-based estimates, and could resolve the present discrepancy between reconstructions based on vegetation and climate models in respect to the mid-Holocene temperature development. At the same time Holocene vegetation changes in the Mediterranean realm are well dated and understood. As a consequence, the Mediterranean region may serve as a role model for understanding the reasons for the deviation of vegetation-based summer temperature reconstructions from the expected insolation-driven temperature trend that is also apparent for other arid to semi-arid regions[4]. Mediterranean vegetation is determined not only by temperature, but to a large extent by the availability and seasonality of moisture[13,14] and human activities such as cultivation, forestry, husbandry, burning and clearcutting that humanized vegetation, creating novel plant communities such as olive, chestnut, walnut and cork-oak woodlands, or promoted disturbance-adapted sclerophyllous vegetation types such as garrigues and maquis[15,16]. These processes can be expected to have affected vegetation-based climate records from at least the

[1]Oeschger Centre for Climate Change Research, University of Bern, Falkenplatz 16, CH-3013 Bern, Switzerland. [2]Institute of Plant Sciences, University of Bern, Altenbergrain 21, CH-3013 Bern, Switzerland. [3]Climate and Environmental Physics, Physics Institute, University of Bern, Sidlerstrasse 5, CH-3012 Bern, Switzerland. [4]Institute of Natural Sciences and Environmental Health, University College of Southeast Norway, N-3800 Bø i Telemark, Norway. [5]Department of Earth Sciences, Vrije Universiteit Amsterdam, De Boelelaan 1085, NL-1081HV Amsterdam, The Netherlands. [6]Institute of Geography, University of Bern, Hallerstrasse 12, CH-3012 Bern, Switzerland. *e-mail: oliver.heiri@ips.unibe.ch

Late Holocene onwards, in the eastern Mediterranean region even as early as the Neolithic period (after about 8000–6000 BC) when first conversions from pristine to humanized vegetation types occurred.

Palaeoclimate reconstructions based on vegetation-independent proxies from Mediterranean landmasses rely on a range of approaches such as stable isotope measurements in lake sediments and speleothems or geochemical analyses of lake sediment records[17–20]. However, most of the records that cover large sections of the Holocene, and that can be used to assess millennial-scale climate variability, are strongly influenced by past changes in humidity. They have therefore been mainly used to qualitatively infer past variations in moisture availability in the region[19,20]. Reconstructions based on lipid biomarkers in marine sediments have produced quantitative records of past temperature change at similar temporal resolution as pollen-based reconstructions and for different sectors of the Mediterranean Sea[18]. Most but not all of these indicate warmer mid-Holocene than late Holocene temperatures[18], in contrast with the available pollen records. However, these reconstructions have been calibrated against sea surface temperature (SST), in many cases annual means[21,22], rather than summer air temperature, although some records apparently mainly reflect temperatures during winter and spring rather than annual averages[23]. Geomorphological evidence of past glacier extent is available for few mountain ranges in the Mediterranean region (for example, the Apennines[17]). Although the disappearance of glaciers in the mid-Holocene has been interpreted as indicating warmer temperatures[17], these records cannot provide fully independent reconstructions of past summer temperature change since glacier extent is influenced by both winter precipitation and summer temperature. Available climate proxy records indicate differences in Holocene trends in available moisture between the western and eastern Mediterranean region[20], as well as more regionally (for example, in the central Mediterranean region) also with latitude[19]. Marine records also suggest some differences in millennial-scale Holocene water temperature changes between the western and southern to eastern Mediterranean regions[18]. For summer temperature records not based on pollen no similar divisions of the Mediterranean region have been reported[18–20].

We present a replicated regional chironomid-based July air temperature reconstruction covering the entire Holocene and parts of the Lateglacial period (∼14,000 years ago to present) from the northern Mediterranean region. Multi-lake studies have demonstrated that the distribution of larval chironomids (non-biting midges) in lakes is strongly related to summer air temperatures[24,25] allowing quantitative temperature reconstructions to be developed from fossil chironomid records. Chironomid-based temperature reconstructions are available from a range of localities in northern, northwest, central and eastern Europe[26–28], and have been used, for example, to validate the performance of climate model runs when inferring Lateglacial summer temperature gradients across Europe[29]. However, for the Mediterranean region chironomid records that cover the entire Holocene and document the timing and amplitude of long-term temperature change during the mid-Holocene are not yet available. Our chironomid records from hydrologically open, non-saline freshwater lakes can be expected to be less sensitive to past changes in precipitation or catchment soil moisture than other available proxy records from Mediterranean landmasses. As long as these lakes maintain some surface outflow, water level changes will not be pronounced. Major increases in salinity or significantly lower water tables would be associated with characteristic shifts in chironomid assemblages[30,31] not observed in our records. Furthermore, for sediment samples obtained from the lake centre, water depth is only a very weak explanatory variable for fossil chironomid assemblage composition, as shown for lakes in the central and northern Alpine region[32], which resemble our study lakes in morphometry, geologic setting and climatic conditions.

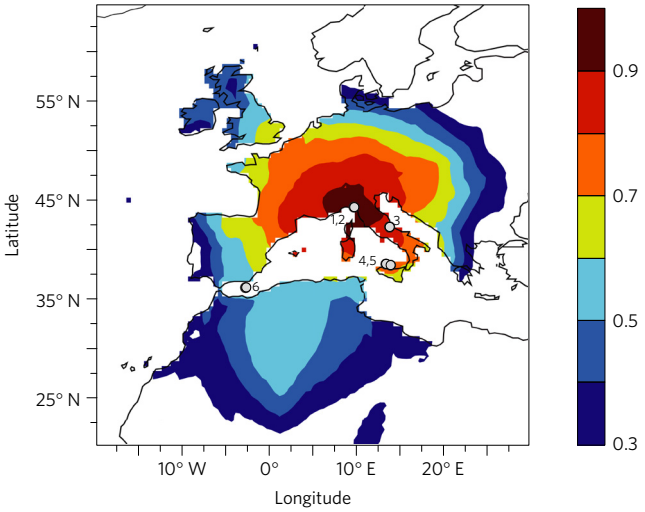

Figure 1 | Location of the Mediterranean proxy records discussed in the text. 1,2: Chironomid records from Verdarolo and Gemini, northern Apennines, Italy. 3: Calderone glacier, southern Apennines, Italy. 4,5: Marine cores BS79-33 and BS79-38 offshore Sicily, Italy. 6: Marine core MD95-2043 offshore southern Spain. Colours indicate how closely interannual July temperature variations at the study sites correlate with the rest of Europe based on the CRU TS3.10 observational data set[45] (as Pearson correlation coefficients between the grid cell at locations 1–2 and the remaining cells in the data set).

New palaeotemperature records

Our new chironomid records come from two mid-elevation lakes, Gemini (Lago Gemini Inferiore, 1,349 m a.s.l.) and Verdarolo (Lago Verdarolo, 1,390 m a.s.l.) in the Tuscan–Emilian Apennines (Fig. 1). The area has been selected since it lies well within the Mediterranean region, with a pronounced seasonally dry climate and Mediterranean vegetation in adjacent lowland regions such as Tuscany to the south, whereas biogeographically the chironomid fauna of the Apennines is similar enough to the Alps to still allow the application of a pan-European chironomid–temperature transfer function that has been extensively tested in the Alpine region[24]. Analyses of instrumental data and climate model runs reveal that at interannual to multidecadal timescales summer temperature variations in the Tuscan–Emilian Apennines (about 44° N, 11° E) are representative for a large section of the northwestern Mediterranean region including the Italian Peninsula between the Alps and Sicily, but also southern France, Corsica and the Julian Alps (Fig. 1 and Supplementary Information). To our knowledge the presented records are the first Italian chironomid-inferred summer temperature reconstructions south of the Po Plain and the first such reconstructions from the Mediterranean region that cover the entire Holocene.

During the Lateglacial period before 11,600 years ago chironomid assemblages at the two lakes were dominated by taxa typical of relatively cool conditions (for example, *Tanytarsus lugens*-type, *Microspectra insignilobus*-type, Fig. 2). At the onset of the Holocene warm-loving taxa expanded such as *Cladotanytarsus mancus*-type, *Tanytarsus pallidicornis*-type, *Microtendipes pedellus*-type and *Chironomus plumosus*-type. During the mid-Holocene, 9,000–5,000 years ago, several warm-adapted chironomid groups reached maximum values, suggesting warm-temperate conditions at the lakes. Finally, in the past 5,000 years a number of warm-loving groups declined again and chironomids indifferent to temperature or adapted to cooler conditions expanded.

We convert shifts in chironomid assemblage composition to estimates of temperature change by using a transfer function that relies on the link between temperature measurements and

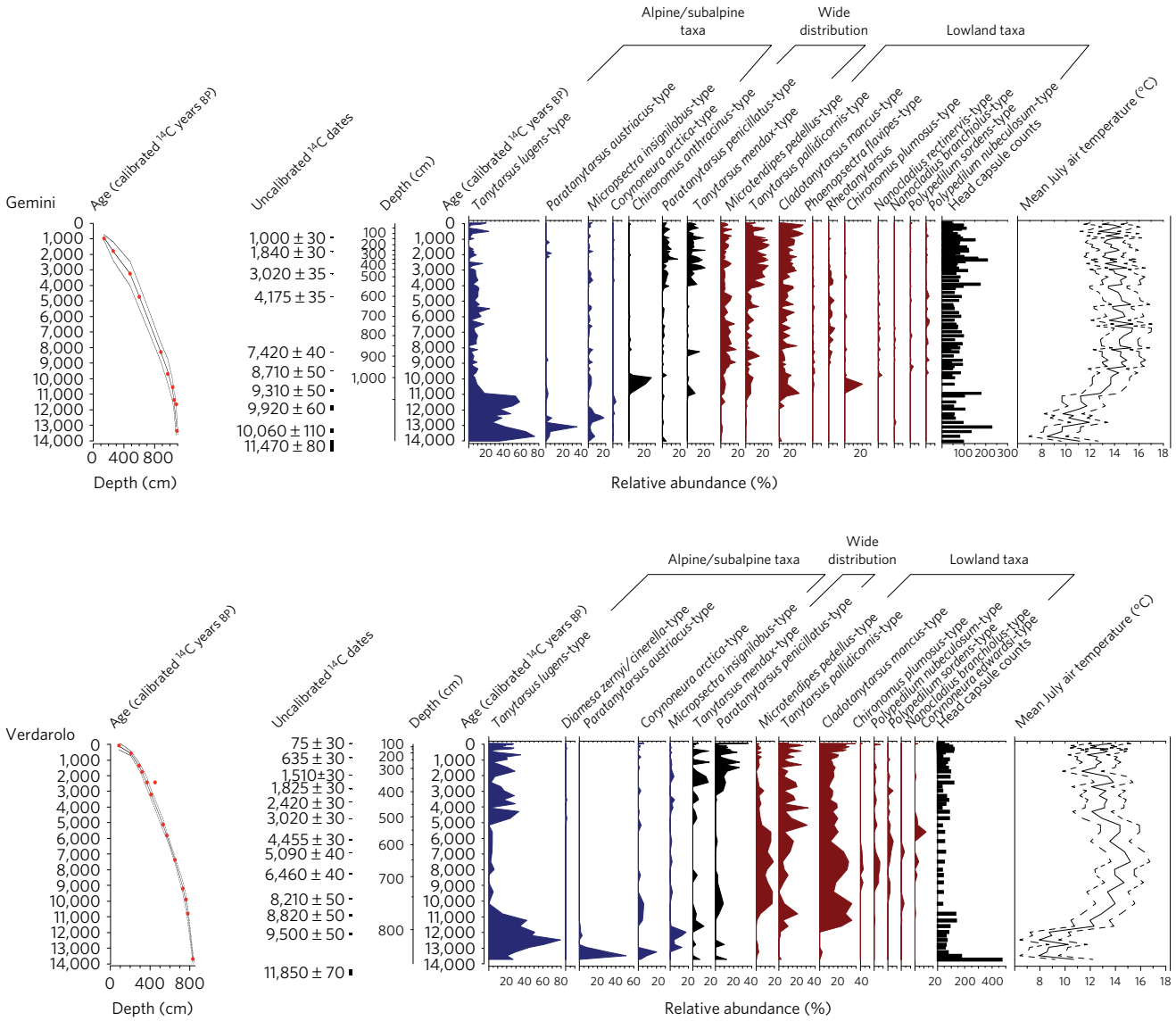

Figure 2 | Fossil chironomid assemblages and chironomid-inferred mean July air temperatures from the Gemini and Verdarolo sediment records. Dominant chironomid taxa, chironomid-inferred mean July air temperatures, the calculated age–depth relationships and the chironomid count sums are indicated. Red and blue colours indicate taxa that, at temperate latitudes, are currently found predominantly in lowland lakes and mountain lakes, respectively[24]. The 95% age confidence intervals and the root mean square error of prediction are indicated for the age-depth relationship and the chironomid records, respectively.

present chironomid communities along a wide climate gradient in Europe[24] (see Methods). Chironomid–temperature transfer functions in the Northern Hemisphere are usually calibrated to mean air temperatures during July, the warmest month in large parts of the northern mid to high latitudes. This allows comparisons of the developed reconstructions with other summer temperature indicators that also provide estimates of July air temperature or are calibrated to temperatures during the warmest month. However, in chironomid–temperature calibration data sets mean July temperature is closely correlated with temperatures during the remaining summer months as well as mean summer (June, July, August) temperature. Available evidence suggests that, rather than to temperature within a particular month, chironomid assemblages respond to temperature during the prolonged (multi-week) period of highest summer air temperatures that determines maximum summer water temperatures in lakes and strongly affects stratification stability, susceptibility to anoxia, lake metabolism and other ecosystem attributes[25]. On the examined spatial and temporal scales these thermal variables are expected to remain closely correlated among each other. Although we present a reconstruction calibrated to mean July air temperature, we therefore consider the results representative for long-term changes in summer air and water temperature in general.

The Gemini and Verdarolo records provide clear evidence for a HTM in inferred July air temperature at the study sites (Fig. 3). At the beginning of the Holocene mean July temperatures increased by ~1.5–4 °C, reaching the pre-industrial temperature levels ~11,000–10,500 years ago. Millennial-scale warming continued until ~9,000 years ago to reach maxima ~1–2 °C higher than during the past 2,000 years. July temperatures remained high during four millennia at both sites. July temperatures gradually declined afterwards, delimiting the HTM to the period 9,000–5,000 years ago. The gradual late Holocene temperature decline ceased only ~2,000 years ago; afterwards reconstructed temperatures remained more or less stable. The Gemini and Verdarolo temperature reconstructions suggest that superimposed on these millennial-scale

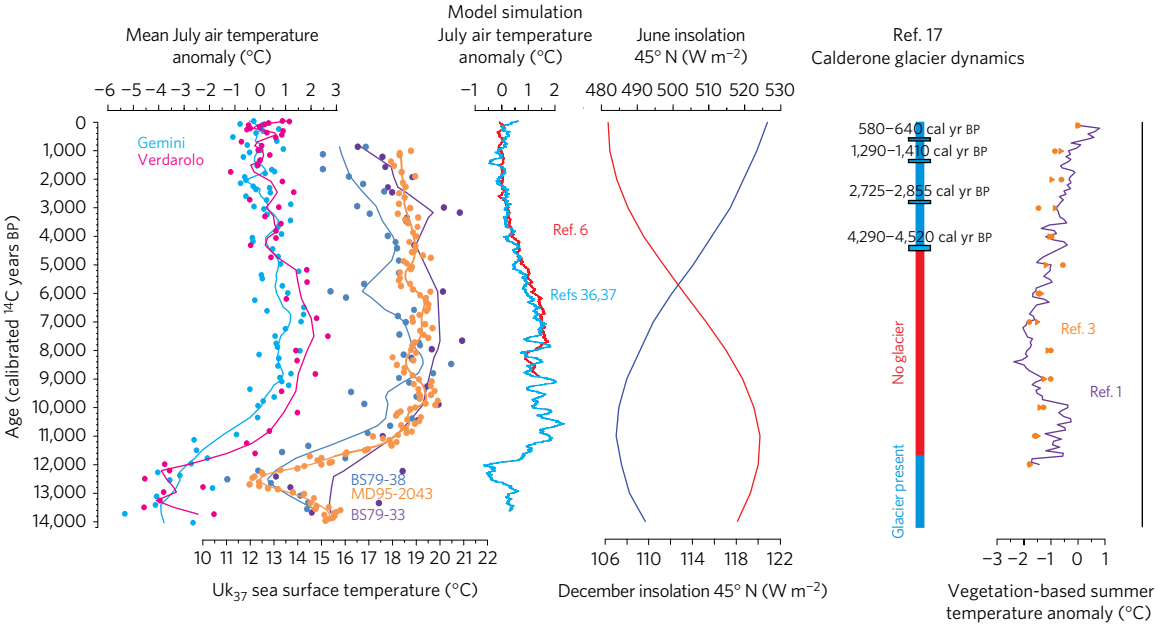

Figure 3 | Chironomid-inferred mean July air temperature for Gemini and Verdarolo compared with other palaeotemperature records. Sea surface temperatures are from western Mediterranean marine cores[21]; modelled temperatures for northern Italy are from the ECBilt-CLIO-VECODE[6] and NCAR CCSM3[36,37] climate models; the reconstructed glacier presence (blue vertical lines) and glacier advances (horizontal bars, with calibrated age intervals) are for the Calderone glacier, Italy[17]. Vegetation-based average temperature anomalies of the warmest month are for southwestern Europe[1]; average summer temperature anomalies[3] are for northern–central Italy (circles) and Europe <45° N (triangles). June (red) and December insolation (blue) is for 45° N (ref. 46). See Methods for calculation of smoothers and anomalies.

trends, centennial oscillations probably occurred (for example, cooling 8,400 to 8,000 years ago). However, the temporal resolution of the time series is too low to thoroughly address this issue.

Mediterranean mid-Holocene thermal maximum

Our temperature reconstructions are in agreement with alkenone records from the western Mediterranean that have been used to estimate mean annual SST. In the Alboran Sea a Holocene SST maximum is reconstructed ~10,000–5,000 years ago[21] (Fig. 3). This pattern is repeated in the Tyrrhenian Sea[21] and agrees with palaeo-glacier evidence from central Italy[17], providing ample and congruent evidence of a thermal maximum in the western and central Mediterranean region during the mid-Holocene. Similarly, summer temperatures were higher during the mid-Holocene than the late Holocene about 200–300 km further north in the nearby Alps[33–35]. In recent Holocene climate model runs[6,36,37] July air temperatures reached maximum values as early as 11,000 years ago, earlier than in our new Italian temperature records and in the Tyrrhenian Sea. However, the model data agree with the chironomid and palaeoceanographic evidence in reconstructing a pronounced early and mid-Holocene warm period and a gradual cooling from 6,000 to 2,500 years ago (Fig. 3).

The cooling trends found in our chironomid records, in the sea and glacier proxies and in the climate model outputs are in line with decreasing summer insolation values, suggesting that orbital forcing was the main determinant of the late Holocene cooling trend in the Mediterranean region. This finding strongly contrasts with pollen-based reconstructions suggesting cooler mid-Holocene summer temperatures in the Mediterranean area compared with present (Fig. 3)[1,3,4]. In Europe, a pronounced contrast between pollen and other proxies is evident mainly for the Mediterranean realm, while for central and northern Europe most proxies including pollen are generally in good agreement in respect to the HTM. Pollen records reconstruct mid-Holocene temperatures on average 1–2 °C cooler than in the late Holocene[1,3]. To reconcile these records with chironomid and SST reconstructions a correction by about 2–4 °C would be necessary, which exceeds the chironomid reconstructions' prediction errors (Fig. 2).

At present, dense forests in the Mediterranean region are restricted to higher elevations where temperatures are cool and moisture availability is high[13]. However, until the intensification of agriculture about 5,000–2,000 years ago such forests including coniferous species were ubiquitous in the Mediterranean lowlands. As a result of human impact through the millennia they were replaced by garrigue and maquis communities[38,39]. For example, on the Italian Peninsula mid-Holocene forests consisted of trees such as *Quercus*, *Abies*, *Fraxinus*, *Ulmus* and *Tilia*[38,40,41]. With intensifying human activity, indicated in palaeorecords by increasing indicators for pasturing and arable farming (for example, cereals) and higher charcoal abundances, dominant tree species disappeared or were markedly reduced (for example, *Abies*, *Tilia*), whereas trees and shrubs that can survive high levels of disturbance (fire, grazing) became dominant elements of the Mediterranean vegetation (for example, *Quercus*, *Olea*, *Chamaerops humilis*, *Erica arborea*, *Pistacia*, *Phillyrea*)[38,39]. These changes had landscape-scale effects on Mediterranean vegetation composition and structure, including a shift in the predominant growth forms (for example, trees versus shrubs and herbs). It is thus likely that pollen-based reconstructions, which rely on present-day abundances or ranges of plants[4], or of plant functional types[1,3], underestimate palaeotemperatures during the natural or quasi-natural conditions before 5,000–2,000 years ago, since the closest modern analogue vegetation for lowland Mediterranean forests in the mid-Holocene is the remnant forest ecosystems at higher altitudes within the Mediterranean region (in the study region above >600–800 m) or in more northern latitudes. Support for this hypothesis comes from ecophysiological modelling experiments that were used to assess mid and late Holocene vegetation trajectories under natural conditions[42]. In addition, it is probable that in the summer-dry Mediterranean climate, vegetation shifts during the mid-Holocene have been primarily controlled by moisture availability instead of temperature[18]. High moisture availability during the mid-Holocene would have promoted vegetation

types that today are associated with cool conditions (for example, mesophilous *Abies* forests)[39]. In agreement with this last interpretation, pollen-based reconstructions for Europe infer substantially cooler mid-Holocene than present summers predominantly for the driest regions[1,3,4]. The amplitude of inferred temperature change is clearly related to variables influencing moisture availability and moisture stress, such as total annual precipitation or precipitation during the driest month (see ref. 4 and Supplementary Information). Lake-level reconstructions in Italy show contrasting humidity trends, while oxygen isotope records suggest moist winter conditions during the mid-Holocene[17,20]. For the Mediterranean region as a whole a range of proxy types suggest higher moisture availability during the mid-Holocene than at present[18], although not all available reconstructions agree with this interpretation[18,20] probably due to the topographic and climatic complexity of the region[20].

Our chironomid-based temperature records, and their agreement with glacier reconstructions and marine records (Fig. 3), imply that Holocene summer temperature reconstructions based on vegetation changes from the Mediterranean region, but also from other semi-arid and seasonally dry regions, may have to be reconsidered. Pollen-based Holocene summer temperature records inferring a cool mid-Holocene originate predominantly from regions with low precipitation or seasonally dry climate, for example, the Mediterranean and the interior of Eurasia or North America[4], where vegetation is expected to be mainly controlled by moisture rather than temperatures during the summer months. In congruence with the Mediterranean evidence, pollen-independent proxies, such as macrofossil-based treeline reconstructions, suggest warmer-than-present summer conditions during the mid-Holocene in some of these regions (for example, interior western North America)[43].

We show that, at least for the northern central Mediterranean region, the Holocene temperature development reconstructed from independent proxy data can be reconciled with the Northern Hemisphere mid-Holocene thermal maximum and late Holocene summer temperature decline inferred by climate model runs if summer temperature proxies are examined that are less influenced by variation in moisture availability than palaeobotanical indicators. There remain minor differences in the exact timing of the HTM between our temperature proxy data and climate model runs, as well as differences in the amplitude and regional expression of mid-Holocene summer warming inferred by different climate models[44]. Nevertheless, our results imply that the major features of the Holocene summer temperature development (HTM, late Holocene cooling) are successfully represented by these models even in the seasonally dry Mediterranean climate. This is in contrast to conclusions of earlier studies comparing pollen-based estimates with climate model-based reconstructions of Holocene summer temperature development[3,8,9].

Methods

Methods, including statements of data availability and any associated accession codes and references, are available in the online version of this paper.

Received 31 August 2016; accepted 6 January 2017; published online 6 February 2017

References

1. Davis, B. A. S., Brewer, S., Stevenson, A. C. & Guiot, J. The temperature of Europe during the Holocene reconstructed from pollen data. *Quat. Sci. Rev.* **22,** 1701–1716 (2003).
2. Peyron, O. *et al*. Holocene seasonality changes in the central Mediterranean region reconstructed from the pollen sequences of Lake Accesa (Italy) and Tenaghi Philippon (Greece). *Holocene* **21,** 131–146 (2011).
3. Mauri, A., Davis, B. A. S., Collins, P. M. & Kaplan, J. O. The climate of Europe during the Holocene: a gridded pollen-based reconstruction and its multi-proxy evaluation. *Quat. Sci. Rev.* **112,** 109–127 (2015).
4. Bartlein, P. J. *et al*. Pollen-based continental climate reconstructions at 6 and 21 ka: a global synthesis. *Clim. Dynam.* **37,** 775–802 (2011).
5. Wanner, H. *et al*. Mid- to Late Holocene climate change: an overview. *Quat. Sci. Rev.* **27,** 1791–1828 (2008).
6. Renssen, H. *et al*. The spatial and temporal complexity of the Holocene thermal maximum. *Nat. Geosci.* **2,** 410–413 (2009).
7. Braconnot, P. *et al*. Evaluation of climate models using palaeoclimatic data. *Nat. Clim. Change* **2,** 417–424 (2012).
8. Fischer, N. & Jungclaus, J. H. Evolution of the seasonal temperature cycle in a transient Holocene simulation: orbital forcing and sea-ice. *Clim. Past* **7,** 1139–1148 (2011).
9. Davis, B. A. S. & Brewer, S. Orbital forcing and role of the latitudinal insolation/temperature gradient. *Clim. Dynam.* **32,** 143–165 (2009).
10. Liu, Z. *et al*. The Holocene temperature conundrum. *Proc. Natl Acad. Sci. USA* **111,** E3501–E3505 (2014).
11. Sala, O. E. *et al*. Biodiversity—Global biodiversity scenarios for the year 2100. *Science* **287,** 1770–1774 (2000).
12. Thuiller, W., Lavorel, S., Araujo, M. B., Sykes, M. T. & Prentice, I. C. Climate change threats to plant diversity in Europe. *Proc. Natl Acad. Sci. USA* **102,** 8245–8250 (2005).
13. Allen, H. D. *Mediterranean Ecogeography* (Pearson Education, 2001).
14. Thuiller, W. *et al*. Large-scale environmental correlates of forest tree distributions in Catalonia (NE Spain). *Glob. Ecol. Biogeogr.* **12,** 313–325 (2003).
15. Roberts, N. *The Holocene: An Environmental History* 2 edn (Blackwell, 1998).
16. Luterbacher, J. *et al*. in *A Review of 2000 Years of Paleoclimatic Evidence in the Mediterranean* (ed. Lionello, P.) 87–185 (Elsevier, 2012).
17. Giraudi, C., Magny, M., Zanchetta, G. & Drysdale, R. N. The Holocene climatic evolution of Mediterranean Italy: a review of the continental geological data. *Holocene* **21,** 105–115 (2011).
18. Abrantes, F. *et al*. *The Climate of the Mediterranean Region—from the Past to the Future* (ed. Lionello, P.) 1–86 (Elsevier, 2012).
19. Magny, M. *et al*. North-south palaeohydrological contrasts in the central Mediterranean during the Holocene: tentative synthesis and working hypotheses. *Clim. Past* **9,** 2043–2071 (2013).
20. Roberts, N., Brayshaw, D., Kuzucuoglu, C., Perez, R. & Sadori, L. The mid-Holocene climatic transition in the Mediterranean: causes and consequences. *Holocene* **21,** 3–13 (2011).
21. Cacho, I. *et al*. Variability of the western Mediterranean Sea surface temperature during the last 25,000 years and its connection with the Northern Hemisphere climatic changes. *Paleoceanography* **16,** 40–52 (2001).
22. Müller, P. J., Kirst, G., Ruhland, G., von Storch, I. & Rosell-Melé, A. Calibration of the alkenone paleotemperature index $U^{K'}_{37}$ based on core-tops from the eastern South Atlantic and the global ocean (60° N–60° S). *Geochim. Cosmochim. Acta* **62,** 1757–1772 (1998).
23. Emeis, K.-C. *et al*. Temperature and salinity variations of Mediterranean Sea surface waters over the last 16,000 years from records of planktonic stable oxygen isotopes and alkenone unsaturation ratios. *Palaeogeogr. Palaeoclimatol. Palaeoecol.* **158,** 259–280 (2000).
24. Heiri, O., Brooks, S. J., Birks, H. J. B. & Lotter, A. E. A 274-lake calibration data-set and inference model for chironomid-based summer air temperature reconstruction in Europe. *Quat. Sci. Rev.* **30,** 3445–3456 (2011).
25. Eggermont, H. & Heiri, O. The chironomid-temperature relationship: expression in nature and palaeoenvironmental implications. *Biol. Rev.* **87,** 430–456 (2012).
26. Brooks, S. J. Fossil midges (Diptera: Chironomidae) as palaeoclimatic indicators for the Eurasian region. *Quat. Sci. Rev.* **25,** 1894–1910 (2006).
27. Moreno, A. *et al*. A compilation of Western European terrestrial records 60–8 ka BP: towards an understanding of latitudinal climatic gradients. *Quat. Sci. Rev.* **106,** 167–185 (2014).
28. Tóth, M. *et al*. Chironomid-inferred Holocene temperature changes in the South Carpathians (Romania). *Holocene* **25,** 569–582 (2015).
29. Heiri, O. *et al*. Validation of climate model-inferred regional temperature change for late- glacial Europe. *Nat. Commun.* **5,** 4914 (2014).
30. Walker, I. R., Wilson, S. E. & Smol, J. P. Chironomidae (Diptera): quantitative palaeosalinity indicators for lakes of western Canada. *Can. J. Fish. Aquat. Sci.* **52,** 950–960 (1995).
31. Heiri, O. Within-lake variability of subfossil chironomid assemblages in shallow Norwegian lakes. *J. Paleolimnol.* **32,** 67–84 (2004).
32. Lotter, A. F., Birks, H. J. B., Hofmann, W. & Marchetto, A. Modern diatom, cladocera, chironomid, and chrysophyte cyst assemblages as quantitative indicators for the reconstruction of past environmental conditions in the Alps. I. Climate. *J. Paleolimnol.* **18,** 395–420 (1997).
33. Tinner, W. & Theurillat, J. P. Uppermost limit, extent, and fluctuations of the timberline and treeline ecocline in the Swiss Central Alps during the past 11,500 years. *Arct. Antarct. Alp. Res.* **35,** 158–169 (2003).

34. Ilyashuk, E. A., Koinig, K. A., Heiri, O., Ilyashuk, B. P. & Psenner, R. Holocene temperature variations at a high-altitude site in the Eastern Alps: a chironomid record from Schwarzsee ob Sölden, Austria. *Quat. Sci. Rev.* **30,** 176–191 (2011).
35. Heiri, O., Tinner, W. & Lotter, A. F. Evidence for cooler European summers during periods of changing meltwater flux to the North Atlantic. *Proc. Natl Acad. Sci. USA* **101,** 15285–15288 (2004).
36. Liu, Z. *et al*. Transient simulation of last deglaciation with a new mechanism for Bølling–Allerød warming. *Science* **325,** 310–314 (2009).
37. Liu, Z. *et al*. Chinese cave records and the East Asia Summer Monsoon. *Quat. Sci. Rev.* **83,** 115–128 (2014).
38. Colombaroli, D., Marchetto, A. & Tinner, W. Long-term interactions between Mediterranean climate, vegetation and fire regime at Lago di Massaciuccoli (Tuscany, Italy). *J. Ecol.* **95,** 755–770 (2007).
39. Tinner, W. *et al*. Holocene environmental and climatic changes at Gorgo Basso, a coastal lake in southern Sicily, Italy. *Quat. Sci. Rev.* **28,** 1498–1510 (2009).
40. Drescher-Schneider, R. *et al*. Vegetation history, climate and human impact over the last 15,000 years at Lago dell'Accesa (Tuscany, Central Italy). *Vegetat. Hist. Archaeobot.* **16,** 279–299 (2007).
41. Tinner, W. *et al*. The past ecology of *Abies alba* provides new perspectives on future responses of silver fir forests to global warming. *Ecol. Monogr.* **83,** 419–439 (2013).
42. Henne, P. D. *et al*. Impacts of changing climate and land use on vegetation dynamics in a Mediterranean ecosystem: Insights from paleoecology and dynamic modeling. *Landsc. Ecol.* **28,** 819–833 (2013).
43. Fall, P. L. Timberline fluctuations and late Quaternary paleoclimates in the Southern Rocky Mountains, Colorado. *Geol. Soc. Am. Bull.* **109,** 1306–1320 (1997).
44. Mauri, A., Davis, B. A. S., Collins, P. M. & Kaplan, J. O. The influence of atmospheric circulation on the mid-Holocene climate of Europe: a data-model comparison. *Clim. Past* **10,** 1925–1938 (2014).
45. Harris, I., Jones, P. D., Osborn, T. J. & Lister, D. H. Updated high-resolution grids of monthly climatic observations – the CRU TS3.10 Dataset. *Int. J. Climatol.* **34,** 623–642 (2014).
46. Berger, A. & Loutre, M. F. Insolation values for the climate of the last 10 million years. *Quat. Sci. Rev.* **10,** 297–317 (1991).

Acknowledgements

Gemini has been cored with permission of the Parco Nazionale Appenino Tosco-Emiliano and Verdarolo with permission of the Parco Regionale Valli del Cedra e del Parma. This study has been supported by the Swiss National Science Foundation (SNF projects PP00P2-114886, 200021_ 134616) and O.H. by the European Research Council (ERC) under the European Union's Seventh Framework Programme (FP/2007–2013) (Starting Grant Project no. 239858).

Author contributions

S.S., O.H. and W.T. conceived the research; S.S. analysed the microfossil data; S.S., O.H., J.F., F.J., H.R. and S.B. designed numerical analyses and S.S., O.H. and F.J. implemented them; all authors contributed to the final interpretation and writing of the manuscript with major contributions by S.S., O.H. and W.T.

Additional information

Supplementary information is available in the online version of the paper. Reprints and permissions information is available online at www.nature.com/reprints. Correspondence and requests for materials should be addressed to O.H.

Competing financial interests

The authors declare no competing financial interests.

Methods

Parallel sediment cores were obtained from the two principal sites, Gemini (44.39° N, 10.05° E) and Verdarolo (44.36° N, 10.12° E), during coring campaigns in 2008 and 2009. Coring took place with a piston corer from a floating platform at the deepest section of the lake basins (2.5 and 2.9 m water depth, respectively) with parallel cores taken at 2 m horizontal distance. Cores were correlated with lithostratigraphic markers to provide continuous sediment sequences for analysis. The chronologies rely on calibrated accelerator mass spectrometry radiocarbon ages from terrestrial plant macrofossils processed at the Poznan Radiocarbon Laboratory (Fig. 2 and Supplementary Methods). All radiocarbon ages were converted to calendar years before present (cal. yr BP) with Calib 7.1 using the INTCAL13 radiocarbon calibration curve[47]. Age–depth models for the 10 dates at Gemini and 14 dates at Verdarolo were established with generalized mixed-effect regression within the framework of generalized additive modelling[48]. At Gemini, all radiocarbon ages provided realistic age estimates (Supplementary Table 1 and Supplementary Fig. 1). At Verdarolo, one date was discarded (449–551 cm, 2,434 calibrated ^{14}C years BP), because further accelerator mass spectrometry dating of plant macrofossils and a comparison with the pollen stratigraphy (unpublished information) indicated that it was contaminated by younger material. Ages between the youngest ^{14}C date and the core top were estimated by linear interpolation to avoid extrapolation to unrealistic ages younger than the coring date.

Chironomid remains were extracted from 0.5–2 cm^3 sediment samples (79 from Gemini and 61 from Verdarolo). Samples were sieved with a 100 μm mesh size sieve and head capsules of chironomid larvae were sorted from the sieve residue under a stereomicroscope (×30–50 magnification), mounted on microscope slides and identified under the compound microscope (×100–400 magnification) on the basis of head capsule morphology[49]. Quantitative chironomid-inferred mean July air temperature estimates from Gemini and Verdarolo were produced by applying a Swiss–Norwegian temperature inference model (based on weighted-averaging partial least-squares regression) to the fossil chironomid records[24]. The model is based on chironomid assemblage data from 274 lakes in the Alpine region and Norway, contains distributional data on most chironomid taxa expected to occur during the late Quaternary in European lake sediments, and predicts mean July air temperature within the calibration data set with a bootstrapped root mean square error of prediction of 1.55 °C. As the two study sites were at high altitudes the reconstructed temperatures were well within the mean July air temperature gradient (3.5–18.4 °C) spanned by the calibration data[24].

Some samples in the Verdarolo and Gemini record were characterized by low count sums. To reach more reliable counts for reconstruction several adjacent samples were therefore merged. This resulted, for Gemini, in a record consisting of 79 samples (Fig. 2), all with count sums within or above the range of minimum count sums of 40–50 head capsules that is commonly used for chironomid-based environmental reconstruction[50–52]. After merging, the Verdarolo record consisted of 38 samples with count sums above 40 head capsules and 12 samples with lower count sums between 30 and 40 head capsules (Fig. 2). The two temperature reconstructions showed consistent results and several studies have shown that, in sediments with very low chironomid concentrations, count sums in the range of 30–40 head capsules can provide acceptable results[53,54]. However, for Verdarolo we also conducted a sensitivity check with further amalgamations resulting in a reconstruction consisting of 43 samples with count sums exceeding 47 head capsules in all instances. Reconstructions at both temporal resolutions revealed the same Holocene July air temperature development, and we therefore retained the 50-sample record with lower head capsule count to maximize the temporal resolution of the Verdarolo record for LOWESS smoothing and for comparison with the climate model results (Fig. 3). Taxa not included in the transfer function were very rare in both records. In the Verdarolo record, overall 0.3% of identified head capsules belonged to taxa not present in the applied inference model, with values per sample ranging from 0–8%. In the Gemini record also 0.3% of identified head capsules were not represented in the transfer function, with values per sample ranging from 0–5%. Error estimates in Fig. 2 indicate the sample-specific cross-validated root mean square error of prediction[55] based on 9,999 bootstrapping cycles. All samples in the chironomid records are within the upper boundary of the 75%/95% confidence intervals of intra-trainingset distances (assessed as both squared chord distance and squared χ^2 distance), thresholds that have been suggested for identifying fossil samples with an unusual combination of taxa not well represented in the calibration data[56]. Our chironomid data set resembles other published late Quaternary chironomid records from central and northwestern Europe[28,57–59] in that there are samples that are both within and beyond the more stringent threshold of the 5th percentile of all trainingset distances. Weighted-averaging partial least-squares regression, the method used for our reconstructions, performs well for samples without very similar modern analogues[60] and other available chironomid records with similar analogue situations generally agree well with expected temperature trends and independent proxy data (see, for example, refs 28,57–59).

Model runs by the National Center for Atmospheric Research Community Climate System Model version 3 (NCAR CCSM3) shown in Fig. 3 are described in refs 36,37 and are driven by atmospheric greenhouse gas concentrations, continental ice sheets and coastlines as well as meltwater flux to the North Atlantic and Gulf of Mexico. NCAR CCSM3 is a coupled atmosphere–ocean general circulation model. The model runs by the ECBilt-CLIO-VECODE model are described in ref. 6 and are driven by orbital parameters, atmospheric greenhouse gas concentrations, continental ice sheets (particularly the Laurentide ice sheet) and meltwater flux. The model is an atmosphere–ocean–vegetation model of intermediate complexity. Whereas the former reconstruction covers the entire Holocene, the ECBilt-CLIO-VECODE reconstruction is available only from 9,000 years onwards. The July air temperatures discussed here are provided for the area 45° ± 2.5° N/11.3° ± 3.75° E and 42°–47° N/5°–15° E, respectively.

Vegetation-based reconstructions shown in Fig. 3 represent average temperature anomalies calculated for different sections of Europe from a large number of pollen records based on a plant functional type modern analogue technique[1,3]. Reconstructed area-averaged temperature anomalies (relative to AD 1890) of the warmest month for the western Mediterranean region (Europe south of 45° N and west of 15° E, curve digitized from the original publication)[1], as well as anomalies of mean summer temperature (relative to AD 1850) based on a European gridded data set provided for 1,000-year time intervals[3] are shown. For the latter data set, averaged values of the grid cells representing central to northern Italy excluding the Alps and the Po Plain (42°–43° N/11°–15° E, 43°–44° N/10°–14° E and 44°–45° N/9°–13° E) and the southern, mainly Mediterranean part of Europe (37°–45° N/11° W–37° E) were selected. Chironomid- and Uk_{37}-based temperatures in Fig. 3 are smoothed with LOWESS smoothers (span 0.1 for Gemini, Verdarolo and MD95-2043, 0.2 for BS79-38, 0.3 for BS79-33), whereas climate model-based temperatures represent 200-year running averages. Temperatures based on climate model runs and the chironomid-inferred temperatures are represented as anomalies relative to the mean temperature of the pre-industrial late Holocene AD 1850 to 2,000 cal. yr BP. Estimates of insolation changes at 45° N (Fig. 3) represent average values for 40° and 50° N as provided in ref. 61 (1978 solution in ref. 46).

Several approaches were used to constrain to what extent the study region (Tuscan–Emilian Apennines) is representative for larger sections of the northern central Mediterranean region and the Italian Peninsula. July air temperatures of the grid cell representing our study sites (44° N, 10° E) were correlated with all European grid cells in the CRU TS3.10 observational data set[45]. The results indicate that within the past 115 years interannual July temperature variability in the study region correlates with temperatures in large sections of the Italian Peninsula, but also in the Po Plain, the northern Adriatic region, southern France, easternmost southern Spain and sections of central Europe (Fig. 1). As instrumental temperature observations are limited to the past one to two centuries, it is not possible to reliably examine spatial correlations in instrumental July air temperature measurements at multidecadal resolution across the northern and central Mediterranean region. Instead we examine the spatial correlations of July air temperatures in the grid cell representing the study region with the rest of Europe in three climate model simulations driven by a range of external forcing factors such as volcanic aerosols, solar variations, and greenhouse gases (ECHO-G simulations[62], CCSM simulations[63], MPI-ESM simulations[64]; see Supplementary Information). These simulations cover the last millennium and were smoothed with a 51-year moving average. The results confirm that also at multidecadal scales variations in July temperature at our study sites are expected to correlate with larger sectors of the northern central Mediterranean region including northern Italy and the Po Plain, the Italian Peninsula, Sicily and southeastern Spain.

Data availability. The chironomid-inferred mean July air temperature records from Gemini and Verdarolo are available at the NOAA National Centers for Environmental Information webpage (https://www.ncdc.noaa.gov/paleo/study/21030). Data from reference 1 (shown in Fig. 3) have been digitized from the original publication. Data from ref. 3 (online resource http://ncdc.noaa.gov/paleo/study/18317), ref. 21 (IGBP PAGES/World Data Center for Paleoclimatology Data Contribution Series no. 2006-106) and ref. 46 (IGBP PAGES/World Data Center for Paleoclimatology Data Contribution Series no. 92-007) have been downloaded from the NOAA National Centers for Environmental Information webpage.

Climate model data from refs 36,37 (shown in Fig. 3) are available at the NCAR climate data webpage (https://www.earthsystemgrid.org/dataset/ucar.cgd.ccsm3.trace.html). Climate model data from ref. 6 can be obtained from H.R. on request.

References

47. Reimer, P. J. *et al*. IntCal13 and MARINE13 radiocarbon age calibration curves 0-50000 years cal BP . *Radiocarbon* **55,** 1869–1887 (2013).
48. Heegaard, E., Birks, H. J. B. & Telford, R. J. Relationships between calibrated ages and depth in stratigraphical sequences: an estimation procedure by mixed-effect regression. *Holocene* **15,** 612–618 (2005).
49. Brooks, S. J., Langdon, P. G. & Heiri, O. The identification and use of Palaearctic Chironomidae larvae in palaeoecology. *Quat. Res. Assoc. Tech. Guide* **10,** 1–276 (2007).

50. Quinlan, R. & Smol, J. P. Setting minimum head capsule abundance and taxa deletion criteria in chironomid-based inference models. *J. Paleolimnol.* **26,** 327–342 (2001).
51. Larocque, I. How many chironomid head capsules are enough? A statistical approach to determine sample size for palaeoclimatic reconstructions. *Palaeogeogr. Palaeoclimatol. Palaeoecol.* **172,** 133–142 (2001).
52. Heiri, O. & Lotter, A. F. Effect of low count sums on quantitative environmental reconstructions: an example using subfossil chironomids. *J. Paleolimnol.* **26,** 343–350 (2001).
53. Larocque, I., Grosjean, M., Heiri, O., Bigler, C. & Blass, A. Comparison between chironomid-inferred July temperatures and meteorological data AD 1850–2001 from varved Lake Silvaplana, Switzerland. *J. Paleolimnol.* **41,** 329–342 (2009).
54. Larocque-Tobler, I., Filipiak, J., Tylmann, W., Bonk, A. & Grosjean, M. Comparison between chironomid-inferred mean-August temperature from varved Lake Zabinskie (Poland) and instrumental data since 1896 AD . *Quat. Sci. Rev.* **111,** 35–50 (2015).
55. Birks, H. J. B., Line, J. M., Juggins, S., Stevenson, A. C. & ter Braak, C. J. F. Diatoms and pH reconstruction. *Phil. Trans. R. Soc. Lond. B* **327,** 263–278 (1990).
56. Francis, D. R., Wolfe, A. P., Walker, I. R. & Miller, G. H. Interglacial and Holocene temperature reconstructions based on midge remains in sediments of two lakes from Baffin Island, Nunavut, Arctic Canada. *Palaeogeogr. Palaeoclimatol. Palaeoecol.* **236,** 107–124 (2006).
57. Muñoz Sobrino, C. *et al*. New data on the Lateglacial period of SW Europe: a high resolution multiproxy record from Laguna de la Roya (NW Iberia). *Quat. Sci. Rev.* **80,** 58–77 (2013).
58. van Asch, N. *et al*. Rapid climate change during the Weichselian Lateglacial in Ireland: chironomid-inferred summer temperatures from Fiddaun, Co. Galway. *Palaeogeogr. Palaeoclimatol. Palaeoecol.* **315–316,** 1–11 (2011).
59. Heiri, O., Lotter, A. F., Hausmann, S. & Kienast, F. A chironomid-based Holocene summer air temperature reconstruction from the Swiss Alps. *Holocene* **13,** 477–484 (2003).
60. Birks, H. J. B. Numerical tools in palaeolimnology—progress, potentialities, and problems. *J. Paleolimnol.* **20,** 307–332 (1998).
61. Berger, A. *Orbital Variations and Insolation Database* IGBP PAGES/World Data Center for Paleoclimatology Data Contribution Series no. 92-007 (NOAA/NGDC Paleoclimatology Program, 1992).
62. Gonzalez-Rouco, J. F., Beltrami, H., Zorita, E. & von Storch, H. Simulation and inversion of borehole temperature profiles in surrogate climates: spatial distribution and surface coupling. *Geophys. Res. Lett.* **33,** L01703 (2006).
63. Hofer, D., Raible, C. C. & Stocker, T. F. Variations of the Atlantic meridional overturning circulation in control and transient simulations of the last millennium. *Clim. Past* **7,** 133–150 (2011).
64. Jungclaus, J. H. *et al*. Climate and carbon-cycle variability over the last millennium. *Clim. Past* **6,** 723–737 (2010).

nature geoscience

SUPPLEMENTARY INFORMATION

DOI: 10.1038/NGEO2891

In the format provided by the authors and unedited.

Warm Mediterranean mid-Holocene summers inferred by fossil midge assemblages

Stéphanie Samartin, Oliver Heiri, Fortunat Joos, Hans Renssen, Jörg Franke, Stefan Brönnimann, Willy Tinner

Supporting online material

This section contains a supporting table, four supporting online Figures and a supporting text section. In Figures S1-S2 the age-depth relationship for Gemini and Verdarolo is presented in more detail than Figure 2 of the main text. Supporting Table 1 lists the uncalibrated and calibrated ^{14}C dates for the records, together with the error estimates for the ages. Figure S3 presents the results of the spatial correlation analyses of the ECHO-G simulations[1], CCSM simulations[2], and MPI-ESM simulations[3] described in the method section. In Figure S4 we provide an example demonstrating that negative mid-Holocene summer temperature anomalies in Europe are predominantly recorded by pollen-based reconstructions from dry regions, as we state in the main text of our article. The presented example is based on a large-scale gridded palaeotemperature dataset based on pollen-data[4] and shows inferred mean anomalies of the temperature of the warmest month for 6000 calibrated ^{14}C years BP (cal. yr BP) relative to modern values. In the supporting text section, finally, we provide a short discussion of the potential effect of early human activities on chironomid records.

Table S1: ^{14}C dates of Gemini (GMC) and Verdarolo (VERA)

Site	Lab. No. Poz-	Depth (cm)	Material	Uncorrected radiocarbon date BP	Cal yr BP (median)*	Cal yr BP 95% limits
GMC	31985	140	Leaves	1000 ± 30	925	799-967
	31986	260	Needles	1840 ± 30	1776	1708-1864
	29367	480.5-482.5	Leaves	3020 ± 35	3216	3078-3343
	29369	599.5-601.5	Leaves, terr. seeds	4175 ± 35	4717	4583-4835
	29370	879-881.5	Needles	7420 ± 40	8258	8176-8341
	32837	970-972	Bark, wood, needles	8710 ± 50	9665	9546-9887
	29366	1033-1035	Indet. branch,	9310 ± 50	10513	10298-10660
	34034	1052-1056	Indet. leaves, wood, bark, indet. CM	9920 ± 60	11341	11271-11610
	34033	1076-1079	Indet. leaves, wood, indet. CM	10060 ± 110	11615	11253-12006
	34032	1081-1089	*Arctostaphylus uva-ursi* leaves, terr. seed	11470 ± 80	13315	13142-13459
VERA	37418	88-90	Leaves	75 ± 30	103	27-259
	32844	208-210	Needles, leaves	635 ± 30	599	553-665
	37420	288-290	Leaves, wood	1510 ± 30	1392	1327-1520
	39388	319	Wood, periderm	1825 ± 30	1765	1634-1862
	32845	368-370	Needles, leaves	2420 ± 30	2446	2351-2696
	39389	410-412	Leaves, wood	3020 ± 30	3215	3080-3340
	37421	449-451	Needles, leaves	2405 ± 35	2434**	2346-2696
	39390	530-531	Wood	4455 ± 30	5123	4965-5286
	32846	568-570	Needles, leaves	5090 ± 40	5818	5743-5917
	37422	649-651	Needles, leaves	6460 ± 40	7371	7289-7434
	32847	728-730	Needles, leaves	8210 ± 50	9175	9019-9394
	39392	760-762	Needles, indet. bud	8820 ± 50	9875	9686-10155
	39393	780-782	Leaves, indet. twig, wood	9500 ± 50	10785	10589-11080
	37423	829-833	Indet. CM, wood, bark, indet. leave fragments	11850 ± 70	13663	13481-13791

Plant macrofossils were AMS dated at the Poznan Radiocarbon Laboratory (Poland). *Calibration of radiocarbon dates: Calib 7.1[5] with INTCAL13 calibration curve[6], Rejected date, CM charred material, Indet. undetermined, terr terrestrial, leaves *Fagus sylvatica*, needle *Abies alba.***

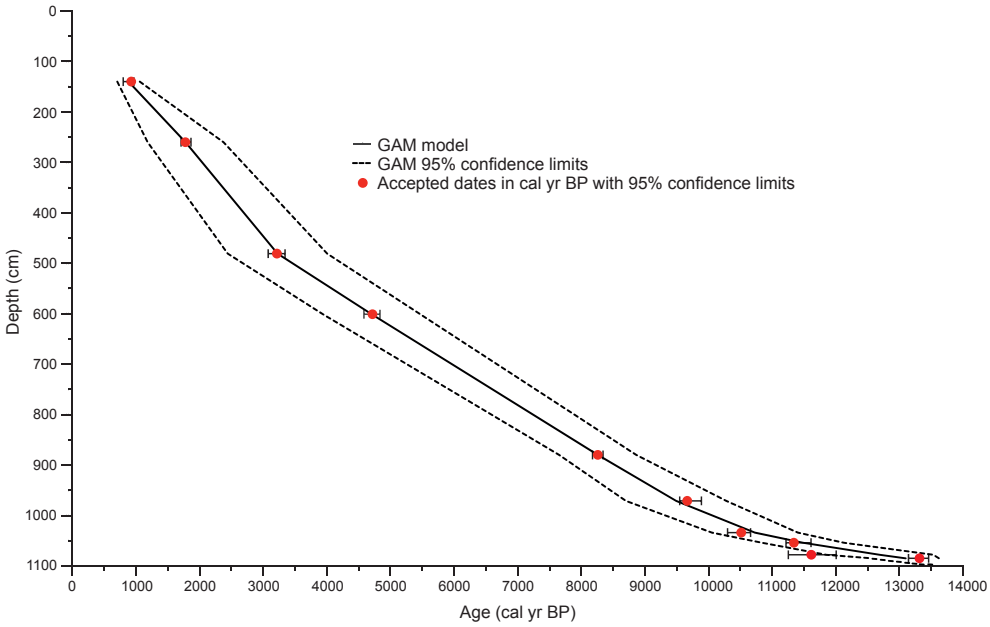

Figure S1. Age-depth model for Gemini. The ^{14}C dates were converted to calibrated years (cal yr BP) with the program Calib version 7.1[5] and the age-depth relationship was developed with generalized additive modeling (GAM)[7].

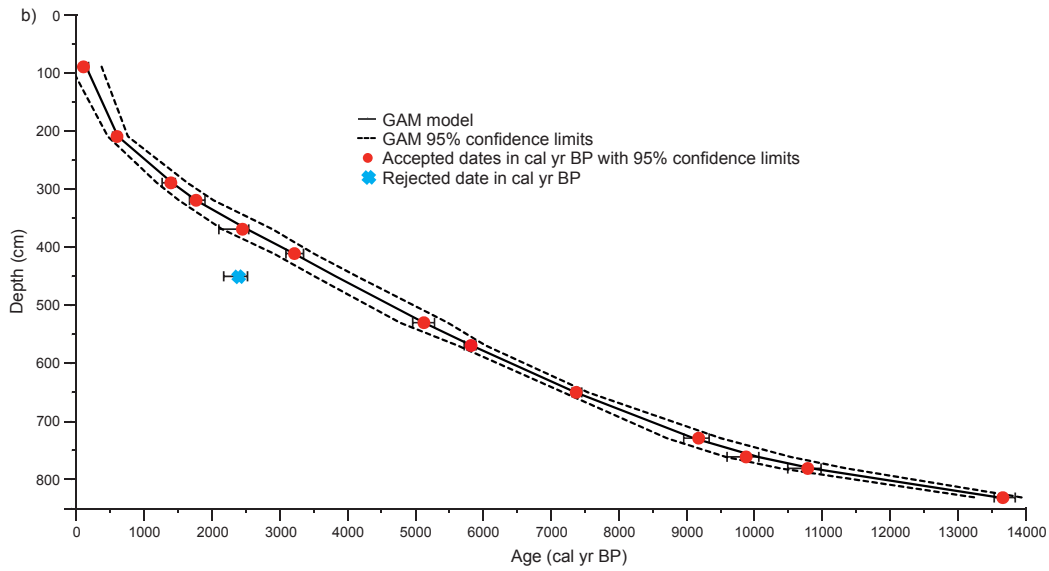

Figure S2. Age-depth model for Verdarolo. The ^{14}C dates were converted to calibrated years (cal yr BP) with the program Calib version 7.1[5] and the age-depth relationship was developed with generalized additive modeling (GAM)[7].

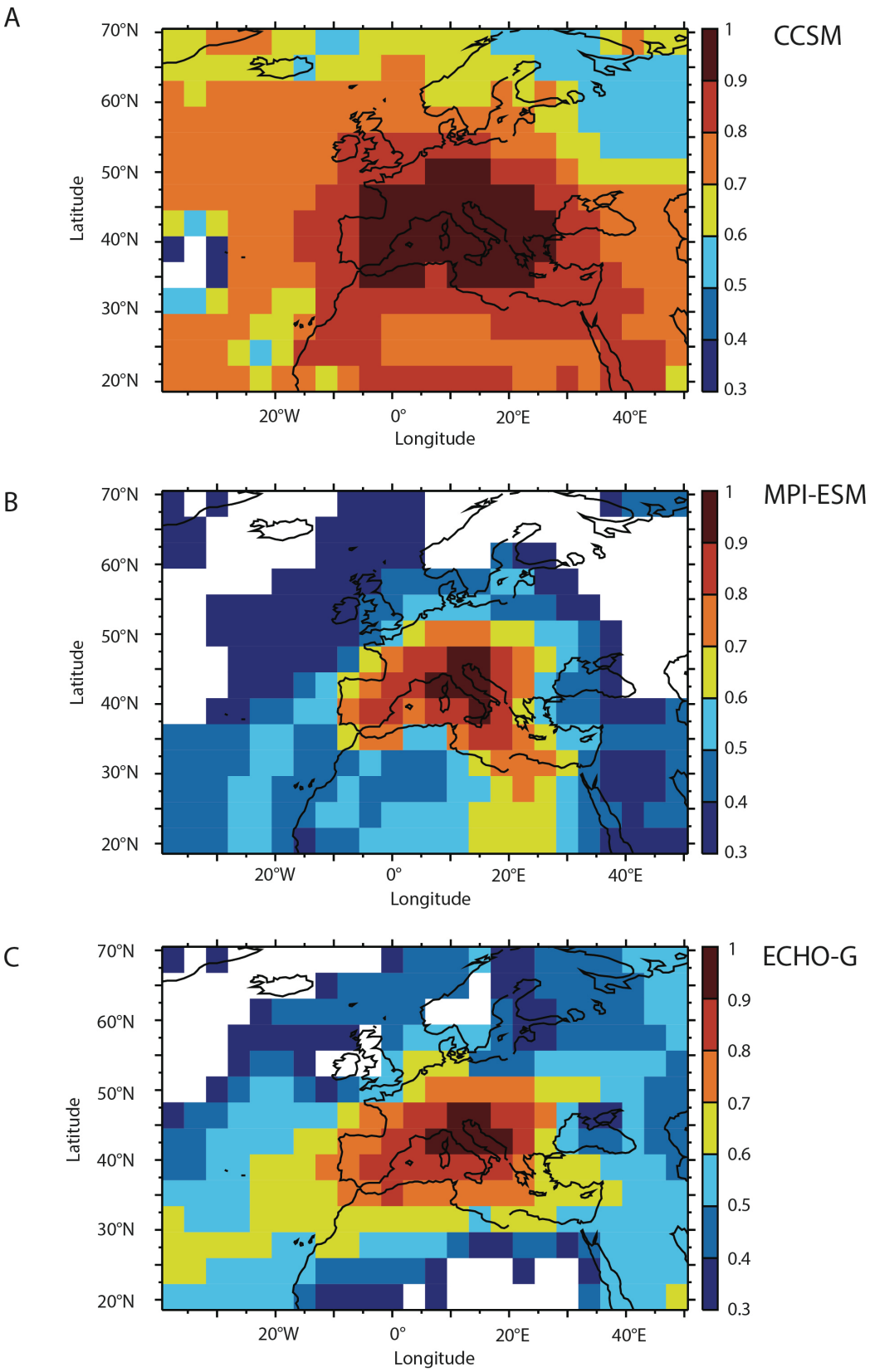

Figure S3. Maps indicating Pearson correlation coefficients between the grid box covering Verdarolo and Gemini and the rest of Europe in the CCSM[2] (A), MPI-ESM[3] (B) and ECHO-G[1] (C) simulations. July temperature has been smoothed with a 51-year moving average to focus on multi-decadal variability.

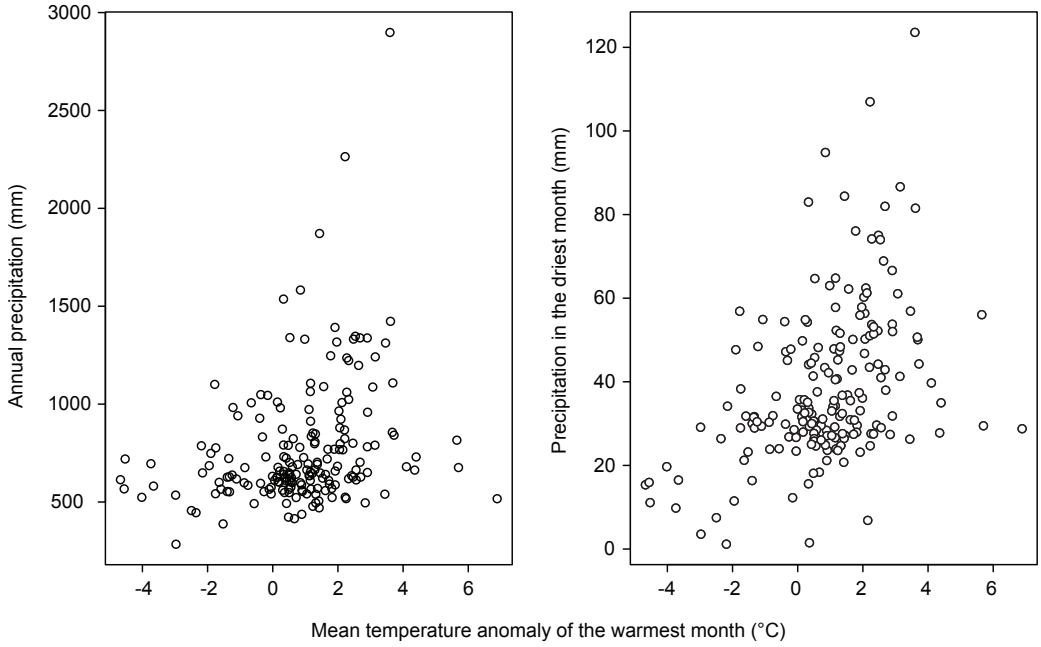

Figure S4. Pollen-inferred mean anomalies of the temperature of the warmest month for 6000 cal. yr. BP in the gridded dataset of Bartlein et al.[4] plotted against modern precipitation values. Pollen-inferred anomalies for Europe (35 to 79°N, -9° to 33°E) are compared with mean annual precipitation and precipitation during the driest month from New et al.[8] Values in the two gridded datasets were matched based on latitude followed by longitude. Average climate values were used if after matching several gridpoints of the New et al.[8] data showed identical offsets in latitude and/or longitude to coordinates in the Bartlein et al.[8] data. Offsets in coordinates up to 1° were accepted and occurred due to differences in the land-sea mask in combination with the different resolutions of the gridded datasets (2°x2° vs 10'x10'). Data are from the IGBP PAGES/World Data Center for Paleoclimatology (Bartlein et al.[4], Data Contribution Series # 2010-127) and the Climatic Research Unit, University of East Anglia, UK (New et al.[8], https://crudata.uea.ac.uk/cru/data/hrg/tmc/).

Effects of human activities on chironomid-inferred temperature records

We argue that pollen-based summer temperature reconstructions in the Mediterranean region have been significantly influenced by human activities during the Late Holocene and probably also, in some regions, as early as the middle Holocene. Chironomid assemblages can also be affected by human activities such as pasturing and clearcutting,[9] which influence nutrient and organic matter transport into lakes. However, in contrast to pollen, chironomids only respond to local human impact whereas pollen-based climate reconstructions are influenced by human activities within a much larger region around lakes due to long distance transport by wind. For Verdarolo a detailed pollen record exists, which indicates that no significant human activities such as clearcutting, arable farming or pasturing occurred in the catchment of the lake prior to 2500 cal. yr. BP, at least not at a scale that this is noticeable in the pollen record and expected to influence the lakes[10]. Sporadic finds of pollen of cultivated plants (e.g. Cerealia, *Cannabis sativa*) suggest that agricultural activities started as early as 4000 cal. yr. BP in the larger region around the lake, most probably in the lowlands south and north of the site (Tuscany, Emilia). Local human activities around the study lakes from 2500 cal. yr. BP onwards could, therefore, potentially have released nutrients and increased the lakes' productivity, favoring chironomid groups typical for warmer summer temperatures[11]. However, both of our chironomid records do not provide any evidence for higher abundances of chironomid groups favored by human activity (e.g. *Chironomus*), or increases in inferred temperatures in the Late Holocene. Similarly, no eutrophication is apparent from the pollen record of Verdarolo (e.g. *Urtica*, aquatic plants). We therefore rule out that the overall trends in inferred July air temperatures and the timing of the HTM in our chironomid records is significantly influenced by human activity in the catchments of the lakes.

References

1 Gonzalez-Rouco, J. F., Beltrami, H., Zorita, E. & von Storch, H. Simulation and inversion of borehole temperature profiles in surrogate climates: spatial distribution and surface coupling. *Geophysical Research Letters* 33, L01703 (2006).

2 Hofer, D., Raible, C. C. & Stocker, T. F. Variations of the Atlantic meridional overturning circulation in control and transient simulations of the last millennium. *Climate of the Past* 7, 133–150 (2011).

3 Jungclaus, J.H. *et al.* Climate and carbon-cycle variability over the last millennium. *Climate of the Past* **6**, 723–737 (2010).

4 Bartlein, P. J. *et al.* Pollen-based continental climate reconstructions at 6 and 21 ka: a global synthesis. *Climate Dynamics* **37**, 775-802, doi:10.1007/s00382-010-0904-1 (2011).

5 Calib 7.1, http://calib.qub.ac.uk/calib/calib.html, accessed June 2015

6 Reimer, P. J. *et al.* IntCal13 and MARINE13 radiocarbon age calibration curves 0-50000 years cal BP. *Radiocarbon* **55**, 1869-1887 (2013).

7 Heegaard, E., Birks, H. J. B. & Telford, R. J. Relationships between calibrated ages and depth in stratigraphical sequences: an estimation procedure by mixed-effect regression. *The Holocene* **15**, 612-618 (2005).

8 New, M., Lister, D., Hulme, M. & Makin, I. A high-resolution data set of surface climate over global land areas. *Climate Research* **21**, 1-25 (2002).

9 Heiri, O. & Lotter, A. F. Holocene and Lateglacial summer temperature reconstruction in the Swiss Alps based on fossil assemblages of aquatic organisms: a review. *Boreas* **34**, 506-516 (2005).

10 Samartin, S. *Chironomid-based environmental and climatic reconstructions for the past 30 000 years from the northern Italian peninsula*. PhD thesis, University of Bern, (2011).

11 Brodersen, K. P. & Quinlan, R. Midges as paleoindicators of lake productivity, eutrophication and hypolimnetic oxgen. *Quaternary Science Reviews* **25**, 1995-2012 (2006).